Regional Studies in Marine Science 101 (2026) 105255

Contents lists available at ScienceDirect

Regional Studies in Marine Science

journal homepage: www.elsevier.com/locate/rsma

Regional patterns of environmental variability in mangrove ecosystems along the southeastern Brazilian coast

Marcelo Antonio Amaro Pinheiro[a,b,1,*], Luis Felipe de Almeida Duarte[c,2], Caio Rodrigues Nobre[d,3], Esli Emanoel Domingues Mosna[a,b,4], Rodrigo dos Santos Rodriguez-Lopes[e,5], Todor Petkov[f,6], Aleksandar Dimitrov[g,7], Dimitrinka Ivanova[g,8]

[a] Universidade Estadual Paulista (UNESP), Campus do Litoral Paulista (CLP), Instituto de Biociências (IB), Departamento de Ciências Biológicas e Ambientais (DCBA) - Grupo de Pesquisa em Biologia de Crustáceos (CRUSTA), Laboratório de Biologia da Conservação de Crustáceos (LBC), Praça Infante Dom Henrique, s/n., Parque Bitaru, São Vicente, SP 11330-900, Brazil
[b] Programa de Pós-Graduação em Ecologia, Evolução e Biodiversidade (PPG-EcoEvioBio), UNESP, Instituto de Biociências, Rio Claro SP, Brazil
[c] Universidade Santa Cecília (UNISANTA) - Pós-graduação em Ciência e Tecnologia Ambiental - Rua Oswaldo Cruz, 277, Boqueirão, Santos, SP 11045-907, Brazil
[d] Universidade Santa Cecília (UNISANTA), Laboratório de Ecotoxicologia, Rua Oswaldo Cruz, 266, Santos, SP 11045-907, Brazil
[e] Programa de Pós-Graduação em Biodiversidade de Ambientes Costeiros (PPG-BAC), UNESP, Instituto de Biociências, Campus do Litoral Paulista, São Vicente SP, Brazil
[f] Faculty of Technical Sciences, Burgas State University "Prof. Dr. Assen Zlatarov", Burgas 8010, Bulgaria
[g] Faculty of Natural Sciences, Burgas State University "Prof. Dr. Assen Zlatarov", Burgas 8010, Bulgaria

ARTICLE INFO

Keywords:
Mangrove ecosystems
Environmental variability
Sediment geochemistry
Trace metals
Biomarkers
Ucides cordatus
Coastal gradients

ABSTRACT

Mangrove ecosystems along the southeastern Brazilian coast are exposed to contrasting degrees of anthropogenic pressure, ranging from industrialized estuarine sectors to relatively preserved protected areas. This study examined regional patterns of environmental variability across six mangrove regions using an integrated dataset of 54 sampling units described by 29 biological, chemical, and sedimentological variables, including sediment-associated metals and biomarkers in the crab *Ucides cordatus*. A Self-Organizing Map (SOM) was used as an exploratory tool to analyze multivariate structure within the dataset. The results revealed a coherent spatial organization consistent with known environmental gradients, distinguishing more impacted central estuaries from southern low-impact mangroves, while partial overlap among adjacent southern regions indicated transitional environmental conditions. Sediment-associated metals, particularly manganese and available copper, were among the main drivers of regional differentiation, together with sediment texture and organic matter. Biomarkers, including neutral red retention time (NRRT) and micronucleus frequency (MN), showed spatial patterns consistent with sediment conditions, suggesting partially distinct cytotoxic and genotoxic responses to environmental variability. These findings demonstrate that integrating sediment geochemistry and biological responses provides a robust framework for describing regional environmental variability and supports the use of *U. cordatus* as a sentinel species in coastal monitoring programs.

* Corresponding author at: Universidade Estadual Paulista (UNESP), Campus do Litoral Paulista (CLP), Instituto de Biociências (IB), Departamento de Ciências Biológicas e Ambientais (DCBA) - Grupo de Pesquisa em Biologia de Crustáceos (CRUSTA), Laboratório de Biologia da Conservação de Crustáceos (LBC), Praça Infante Dom Henrique, s/n., Parque Bitaru, São Vicente, SP 11330-900, Brazil.

E-mail addresses: marcelo.pinheiro@unesp.br (M.A.A. Pinheiro), duarte.mepi@gmail.com (L.F.A. Duarte), caio.biomar@gmail.com (C.R. Nobre), e.mosna@unesp.br (E.E.D. Mosna), rodrigo.rodriguez@unesp.br (R.S. Rodriguez-Lopes), todor-petkov@uniburgas.bg (T. Petkov), adimitrov@uniburgas.bg (A. Dimitrov), divanova@btu.bg (D. Ivanova).

[1] 0000-0003-0758-5526
[2] 0000-0002-4658-4684
[3] 0000-0001-6626-3354
[4] 0000-0002-6330-1586
[5] 0009-0000-8580-4021
[6] 0000-0003-0411-4956
[7] 0000-0002-2683-2222
[8] 0000-0002-3239-4257

https://doi.org/10.1016/j.rsma.2026.105255
Received 29 March 2026; Received in revised form 31 May 2026; Accepted 13 July 2026
Available online 14 July 2026

1. Introduction

Mangrove forests are among the most productive and ecologically important coastal ecosystems worldwide, providing essential services such as shoreline stabilization, nutrient cycling, carbon sequestration, and biodiversity support (Duke et al., 2007; Alongi, 2014; Schaeffer-Novelli et al., 2023; Khan et al., 2025). As transition zones between terrestrial and marine environments, they function as efficient biogeochemical filters, regulating material fluxes and sustaining complex trophic networks (Souza et al., 2018; Souza and Pinheiro, 2022; Albertin-Santos et al., 2025).

Despite their ecological and socioeconomic importance, mangroves have experienced a marked global decline driven by urbanization, industrial activities, and land-use change (Friess et al., 2019; Pinheiro et al., 2022; Heck et al., 2024). These pressures are particularly intense in tropical regions, where impacts are often chronic and spatially heterogeneous (Heck et al., 2024; IUCN, 2024).

A key characteristic of mangrove systems is their capacity to retain contaminants, especially trace metals, within fine-grained, organic-rich sediments (Tognella et al., 2022; Ramos et al., 2024; Zhang et al., 2025). Although this process can reduce contaminant export to adjacent waters, it increases resident organisms' exposure to sediment-associated pollutants (Duarte et al., 2025). Such exposure may induce sublethal effects, including cytotoxicity and genotoxicity, potentially affecting organism fitness before visible ecological degradation occurs (Duarte et al., 2016; Duarte et al., 2017).

These characteristics make mangroves suitable for integrative environmental assessments combining chemical, sedimentological, and biological indicators. In this context, the mangrove crab *Ucides cordatus* (Linnaeus, 1763) is a key model species in the Western Atlantic (Pinheiro et al., 2017). As an ecosystem engineer, it influences sediment structure and nutrient cycling through burrowing and feeding activities (Kristensen, 2008). Its close association with sediments, ecological relevance, and relatively long lifespan make it particularly suitable as a sentinel species (Pinheiro et al., 2005; Pinheiro, 2026). Cytotoxic and genotoxic biomarkers in this species provide early-warning signals of environmental stress across spatial and temporal scales (Duarte et al., 2016, 2019; Pinheiro et al., 2022).

Mangrove ecosystems along the southeastern Brazilian coast form a well-defined environmental gradient, ranging from highly impacted estuarine systems to relatively preserved protected areas. Although previous studies in this region have documented differences in sediment quality, metal contamination, and biological responses, these components have often been analysed separately or using linear approaches, such as Principal Component Analysis (PCA) used by Duarte et al. (2016), which limits the ability to capture gradual transitions and multivariate interactions among ecosystem compartments.

The environmental gradients investigated in this study were characterized using an integrated set of biological, geochemical, and sedimentological descriptors that are widely employed in mangrove environmental assessments and monitoring programs (N'goran et al., 2022; Adam et al., 2023; Rinehart et al., 2024; Swetha et al., 2025). Together, these descriptors provide complementary information on environmental quality and ecosystem condition across multiple levels of biological organization.

To address this complexity, exploratory multivariate tools can help summarize such datasets and identify coherent spatial patterns without imposing predefined classifications. Self-Organizing Maps (SOMs) have been applied in environmental studies to identify patterns and gradients in high-dimensional data (Kohonen, 2001; Fusco and Perez, 2019; Guagliardi et al., 2022; Licen et al., 2023; Hussain et al., 2024), particularly in systems where gradual environmental transitions complicate the identification of discrete ecological boundaries.

Previous assessments in this region have primarily relied on linear ordination techniques, such as Principal Component Analysis (PCA), to relate biological responses of *Ucides cordatus* to environmental gradients (Duarte et al., 2016; Pinheiro et al., 2017). Although effective, these approaches may not fully capture nonlinear relationships and transitional environmental conditions typical of estuarine systems. Furthermore, whether integrated biological, geochemical, and sedimentological descriptors can consistently characterize regional environmental gradients across mangrove ecosystems remains insufficiently explored along the southeastern Brazilian coast.

Accordingly, this study examines regional patterns of environmental variability across six mangrove regions along the southeastern Brazilian coast using an integrated set of biological, chemical, and sedimentological variables, with Self-Organizing Maps (SOM) applied as an exploratory analytical tool. Our main hypothesis is based on the prediction that SOM would distinguish more impacted central estuarine regions from southern mangroves with comparatively low impact, in addition to observing transition gradients in adjacent regions, presenting similar sedimentary and biogeochemical characteristics. By integrating abiotic variables and biological responses, this approach aimed to evaluate whether the biomarkers and population descriptors of *U. cordatus* provide ecologically significant signals along these regional environmental gradients.

2. Materials and Methods

2.1. Study areas

This study was conducted in six mangrove regions along the coast of São Paulo State, Southeastern Brazil, encompassing estuarine systems with contrasting levels of anthropogenic pressure and conservation status (Fig. 1). Together, these regions form a well-defined gradient of anthropogenic influence, geomorphological settings, and biogeochemical conditions, providing an appropriate spatial framework for multivariate environmental assessment and for evaluating the ability of Self-Organizing Maps (SOM) to discriminate between contrasting and transitional ecological states in mangrove ecosystems. The six mangrove regions are briefly characterized below by their dominant anthropogenic pressures, sedimentary settings, and biogeochemical features, which collectively define the environmental gradient examined in this study.

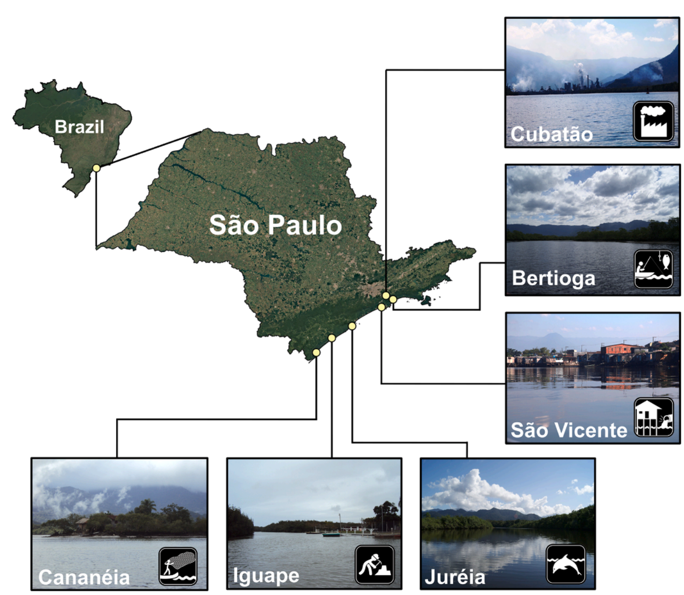

Fig. 1. Location of the six mangrove regions sampled along the coast of São Paulo State, southeastern Brazil. The study area comprises 18 subareas distributed across the central and southern coastal sectors. The map was redesigned by Gustavo Pinheiro and Esli Mosna; photographs were obtained from the CRUSTA collection (Marcelo Pinheiro, UNESP, IB/CLP).

(1) **Bertioga (BET).** Bertioga comprises estuarine mangroves subject to moderate anthropogenic influence, primarily from urban runoff and legacy contamination from a former municipal landfill near the sampling sectors. Periodic increases in Cu and Pb concentrations in water and surface sediments indicate diffuse contamination pathways, which may vary seasonally according to rainfall-driven runoff, tidal exchange, and terrestrial inputs, rather than reflecting persistent industrial discharges (CETESB, 2021; Timoszczuk et al., 2026). Mangrove forests exhibit intermediate structural development, and sediments are composed of a mixed fine-to-medium matrix shaped by tidal exchange and terrestrial inputs.

(2) **Cubatão (CUB).** This region is the most industrialized area investigated and has historically been exposed to high levels of emissions from the metallurgical, petrochemical, fertilizer, and steel industries. Long-term accumulation of trace metals, particularly Cd, Pb, Cu, and Hg, has been extensively documented in estuarine and mangrove sediments (CETESB, 2021; Gonçalves et al., 2012). Despite chronic contamination, mangrove forests remain tall and structurally developed, reflecting continuous exposure to atmospheric deposition and industrial effluent inputs.

(3) **São Vicente (SAV).** Located within the same estuarine complex as Cubatão, São Vicente receives contaminants redistributed by tidal circulation and is bordered by extensive informal waterfront settlements (stilt houses), which contribute additional diffuse urban inputs. Elevated concentrations of Hg and other trace metals in sediments have been reported, particularly at sampling points within this sector (Kim et al., 2022). These conditions are associated with pronounced genotoxic responses in *Ucides cordatus* (Duarte et al., 2016; Pinheiro et al., 2021). Sediments are heterogeneous, and mangrove stands display moderate structural complexity.

(4) **Iguape (IGU).** This region lies within the lower Ribeira de Iguape estuary and has historically been influenced by upstream mining activities, resulting in the enrichment of Mn, Cu, and Hg in estuarine sediments (Mahiques et al., 2009). These legacy inputs persist in contaminated sediments and have been associated with ecotoxicological effects (Perina and Abessa, 2020). Fluvial-dominated hydrodynamics favor deposition of fine, organic-rich sediment, enhancing metal retention and supporting moderately developed mangrove forests.

(5) **Cananéia (CAN).** Located in the southern sector of the Cananéia–Iguape estuarine–lagoon complex, this region exhibits low levels of contamination, and trace metal distributions are largely controlled by natural geochemical processes, with local Mn enrichment linked to sedimentary dynamics (Millo et al., 2021). Nutrient-poor sediments and reduced anthropogenic pressure support its designation as a low-impact southern reference area.

(6) **Juréia (JUR).** The Juréia–Itatins Ecological Station (JIES) represents the low-impact endmember of the environmental gradient. Metal concentrations in water, sediments, and *Ucides cordatus* remain at baseline levels, confirming its role as an ecological control site (Pinheiro et al., 2013; Pinheiro et al., 2021). Mangroves occur within an intact landscape characterized by undisturbed hydrology and negligible external inputs.

Together, these six regions encompass a broad spectrum of environmental conditions, ranging from heavily industrialized estuaries to fully preserved mangrove forests, allowing robust evaluation of SOM performance in detecting transitional environmental conditions.

2.2. Environmental variables and data structure

Prior to the Self-Organizing Map analysis, the dataset was examined through a sequence of exploratory and integrative analyses to characterize environmental gradients rather than to test isolated hypotheses. Following the approach of Duarte et al. (2016), biological responses, sedimentological properties, and geochemical variables were first evaluated descriptively to assess their spatial variability and ecological relevance across mangrove regions. The joint behavior of variables was then considered within a multivariate framework, acknowledging their strong interdependence in mangrove ecosystems.

All variables were collected during a single sampling campaign, minimizing temporal variability. Each mangrove region was represented by three subareas to ensure adequate spatial coverage. Within each subarea, three 5 × 5 m square plots were randomly established, for a total of nine sampling units per region. In total, 54 sampling units were analyzed. All environmental, sedimentological, chemical, and biological measurements were spatially matched at the plot level, following the sampling design detailed by Duarte et al. (2016).

The SOM analysis was based on 29 biological, chemical, and sedimentological variables summarized in Table 1. These variables include biological responses (cytotoxic and genotoxic biomarkers: NRRT and MN, respectively), sediment-associated metal concentrations, grain-size fractions, and sediment geochemical attributes, which are widely employed as indicators of environmental quality in mangrove ecosystems (Marchand et al., 2006; Alongi, 2014; Duarte et al., 2016).

The selection of variables aimed to capture interactions among ecosystem compartments rather than isolated stressors, thereby reflecting the integrated nature of mangrove biogeochemical functioning. This multivariate structure is well-suited to SOM analysis, enabling the identification of complex environmental patterns in high-dimensional datasets (Guagliardi et al., 2022; Licen et al., 2023).

The complete dataset used for SOM training and evaluation, including raw standardized values, is provided in Supplementary Tables S1–S4.

2.3. Self-Organizing Map analysis

Self-Organizing Maps were applied as an unsupervised multivariate tool to explore spatial and environmental patterns across the six mangrove regions. The dataset comprised 54 samples (nine per region), each described by 29 variables. Although the number of variables relative to the sample size may appear comparatively high, SOM algorithms are specifically designed to handle complex multivariate structures and high-dimensional environmental datasets by projecting them onto a lower-dimensional topology while preserving neighborhood relationships among samples (Kohonen, 2001; Atanassov and Sotirov, 2006; Licen et al., 2023; Sotirov et al., 2023).

A two-dimensional SOM topology (3 × 2) was defined, resulting in six neurons corresponding to the number of geographical regions investigated. This configuration was intentionally selected to facilitate ecological interpretation and direct comparison between SOM-derived clusters and known regional classifications rather than to maximize computational resolution (Hua and Anderson-Frey, 2022; Licen et al., 2023).

The SOM was trained for 1000 iterations using a competitive learning algorithm based on Kohonen (2001) and subsequent optimization approaches (Atanassov and Sotirov, 2006). During training, weight updates were applied using a neighborhood function centered on the best-matching unit:

$$w_i(q) = w_i\,(q-1) + \alpha\,[p(q) - w_i\,(q-1)]$$

where $\boldsymbol{w_i(q)}$ represents the weight vector of neuron $\boldsymbol{i}$ at iteration $\boldsymbol{q}$; $\boldsymbol{w_i}$ $\boldsymbol{(q-1)}$ is the weight vector from the previous iteration; $\boldsymbol{p(q)}$ is the input vector at iteration $\boldsymbol{q}$, and $\boldsymbol{\alpha}$ is the learning rate. Model configuration and training procedures followed standard approaches described in the SOM literature, with particular emphasis on environmental and ecological applications (Hagan et al., 2014; Guagliardi et al., 2022; Du et al., 2022; Licen et al., 2023).

Table 1
Environmental, toxicological, biological, and sediment-related variables used as input for the Self-Organizing Map (SOM). For each variable, analytical description, measurement unit, environmental matrix, and ecological relevance are provided.

Variable	Description	Unit	Environmental matrix	Ecological relevance
NRRT	Neutral Red Retention Time	min	Biota (*U. cordatus*)	Cytotoxic stress
MN	Micronucleus frequency	‰	Biota (*U. cordatus*)	Genotoxic damage indicator
CRAB	Crab density	ind. m^{-2}	Biota (*U. cordatus*)	Benthic activity
Cu.Sed	Copper	$\mu g\ g^{-1}$	Sediment	Indicator of urban contamination
Pb.Sed	Lead	$\mu g\ g^{-1}$	Sediment	Indicator of historical contamination
Cd.Sed	Cadmium	$\mu g\ g^{-1}$	Sediment	Toxic trace metal
Mn.Sed	Manganese	$\mu g\ g^{-1}$	Sediment	Redox-sensitive element
Cr.Sed	Chromium	$\mu g\ g^{-1}$	Sediment	Industrial background
Hg.Sed	Mercury	$ng\ g^{-1}$	Sediment	Toxic trace metal
CS	Coarse sand	$g\ kg^{-1}$	Sediment	Sediment structure
MS	Medium sand	$g\ kg^{-1}$	Sediment	Hydrodynamics
FS	Fine sand	$g\ kg^{-1}$	Sediment	Depositional energy
VFS	Very fine sand	$g\ kg^{-1}$	Sediment	Metal retention
SIL	Silt	$g\ kg^{-1}$	Sediment	Contaminant binding
CLA	Clay	$g\ kg^{-1}$	Sediment	Metal adsorption
pH	Sediment pH ($CaCl_2$)	–	Sediment	Metal solubility
OM	Organic matter	$g\ dm^{-3}$	Sediment	Nutrient cycling
P	Phosphorus	$mg\ dm^{-3}$	Sediment	Eutrophication
K	Potassium	$mmolc\ dm^{-3}$	Sediment	Soil fertility
Ca	Calcium	$mmolc\ dm^{-3}$	Sediment	Buffering capacity
Mg	Magnesium	$mmolc\ dm^{-3}$	Sediment	Mineral composition
Al	Aluminum	$mmolc\ dm^{-3}$	Sediment	Acidity indicator
H + Al	Potential acidity	$mmolc\ dm^{-3}$	Sediment	Soil acidity
B	Boron	$mg\ dm^{-3}$	Sediment	Marine influence
Cu	Available copper	$mg\ dm^{-3}$	Sediment	Bioavailable metal
Fe	Iron	$mg\ dm^{-3}$	Sediment	Redox control
Mn	Manganese	$mg\ dm^{-3}$	Sediment	Biogeochemical cycling
Zn	Zinc	$mg\ dm^{-3}$	Sediment	Trace metal
S-SO4	Sulphate	$mg\ dm^{-3}$	Sediment	Sulphur cycling

All SOM analyses were implemented in R (version 4.4.1; R Core Team, 2024) using the kohonen package (v. 3.0.12; Wehrens and Buydens, 2007; Wehrens and Kruisselbrink, 2023). Prior to training, all variables were standardized using z-score normalization. No log-transformation was applied before standardization. The SOM was trained on a hexagonal grid (3 × 2) for 1000 iterations (*rlen* = 1000) with an initial learning rate of 0.05 and an initial neighborhood radius of 1.0, both decreasing linearly during training. Alternative SOM topologies (2 × 3 and 4 × 2) were also explored, and the 3 × 2 configuration was retained because it provided an appropriate balance between topological representation and ecological interpretability.

To evaluate the quality of the trained SOM, two standard internal performance metrics were calculated: the quantization error (*QE*), which measures the average distance between input vectors and their corresponding best-matching units, and the topographic error (*TE*), which evaluates the preservation of topological relationships in the map (Kohonen, 2001; Licen et al., 2023). These metrics provide complementary indicators of map resolution and topology preservation, enabling assessment of the adequacy of the selected SOM configuration.

Visualization of SOM outputs, including hit maps, component planes, confusion matrices, and the U-matrix, was performed in R using functions from the ***kohonen***, ***ggplot2***, and ***reshape2*** **packages**.

Cluster identity was assigned based on the predominant geographic origin of samples mapped to each neuron. Specifically, the most frequent regional label associated with each neuron was used to define its representative region, allowing evaluation of classification performance without imposing predefined class boundaries during training. Because cluster identity was defined a posteriori based on the predominant geographical origin of samples mapped to each neuron, classification accuracy should be interpreted as an internal measure of agreement between SOM-derived clusters and regional environmental patterns, rather than as a predictive validation. Consequently, biological signatures were inferred not only from the accuracy of the classification model, but also from verifying the component planes and weight distributions of the biological descriptors in the topology of the trained SOM.

Model performance and interpretability were further assessed by examining the distribution of samples across neurons, component planes, and classification patterns.

3. Results

The Self-Organizing Map (SOM), trained with 54 samples described by 29 biological, chemical, and sedimentological variables (Table 1), revealed a clear multivariate structure among mangrove environments along the coast of São Paulo State. Samples were organized into six neurons forming regional groupings that reflected gradients of anthropogenic influence, sediment characteristics, and geochemical conditions (Fig. 2A). The SOM hit map showed a strong concentration of samples from the CAN region within a single neuron, indicating a distinct environmental profile relative to the other regions. The trained SOM exhibited a quantization error (*QE*) of 3.33 and a topographic error (*TE*) of 0.259, indicating an adequate representation of the dataset's multidimensional structure.

Inspection of the component planes indicated that the neuron containing the majority of samples from the CAN region was associated with elevated values of several sedimentary and chemical variables, suggesting that this region occupies a distinct position along the environmental gradient represented in the SOM (Fig. 2A, B). In particular, sediment-associated metals contributed substantially to the spatial differentiation between regions (Fig. 2B). Based on the numerical weighting ranges derived from the SOM model (Table 2), manganese (Mn) and available copper (Cu) showed the greatest variability in the SOM grid, with weighting ranges of 3.09 and 2.92 and standard deviations of 1.19 and 1.13, respectively. In contrast, aluminium (Al), iron (Fe), and magnesium (Mg) showed narrower weight ranges (1.15–1.58), possibly indicating a comparatively homogeneous geochemical background throughout the study area, suggesting a lithogenic or sedimentary matrix-related signal, which may be related to the lower contribution of these variables to regional differentiation.

Sediment texture and organic matter also contributed to the multivariate structure identified by the SOM. Fine-grained sediment fractions (fine and very fine sand, silt, and clay) and organic matter displayed relatively high weight amplitudes, reflecting their importance in distinguishing depositional settings among regions (Fig. 2B). Overall, 79.3% (23 of 29) of the input variables showed weight ranges greater than 2.0, confirming the combined influence of biological, chemical, and sedimentological descriptors on SOM organization (Table 2).

In addition to abiotic drivers, biological descriptors of the crab *Ucides*

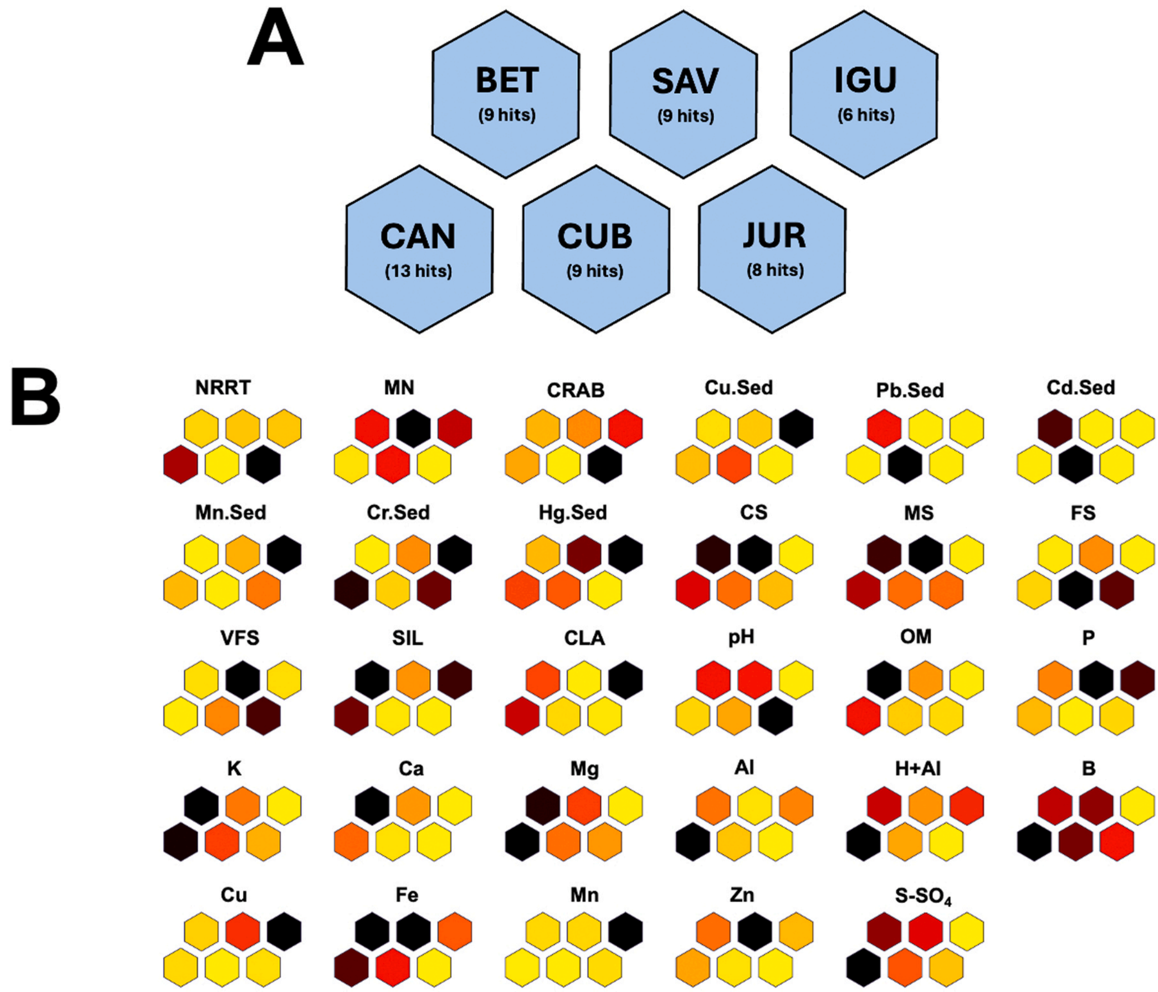

Fig. 2. Self-Organizing Map (SOM) results illustrating the multivariate organization of the studied mangrove regions. (A) SOM hit map showing the distribution of samples across the six neurons of the hexagonal SOM grid (3 × 2). Each hexagon represents one neuron, and numbers indicate the number of samples assigned to each neuron (hits). (B) Component planes for the 29 environmental variables used in the SOM analysis, showing their relative distribution across neurons after z-score normalization. Colors range from low values (yellow) to high values (dark red to black). Color scales are independently standardized for each variable and therefore represent relative variation within each component plane rather than direct comparisons among variables.

cordatus contributed to the multivariate structure. Component planes revealed substantial variability for toxicological biomarkers, with weight ranges of 2.37 for neutral red retention time (NRRT) and 2.18 for micronucleus frequency (MN) (Table 2). Although both biomarkers followed a similar spatial gradient, their weight distributions differed across neurons, indicating partially distinct contributions to the SOM structure. Crab density (CRAB) also contributed to ecosystem differentiation, with a weight range of 1.60, indicating a comparatively smaller but consistent influence across the network.

The agreement between SOM-derived clusters and the geographical origin of samples, evaluated through a confusion matrix, reached an overall concordance of 85.2%, with 46 of the 54 samples associated with the cluster representing their region of origin (Fig. 3). Bertioga (BET), Cubatão (CUB), and São Vicente (SAV) showed complete agreement (100%). Lower values were observed for Iguape (IGU; 66.7%), Cananéia (CAN; 77.8%), and Juréia (JUR; 66.7%), with misclassifications occurring primarily between IGU and CAN and between CAN and JUR. These results indicate a strong correspondence between SOM-derived clusters and the geographical origin of samples, although these values should be interpreted as an internal measure of concordance rather than predictive accuracy, since cluster labels were assigned *a posteriori* based on the dominant regional membership of samples mapped to each neuron.

The U-matrix representation was used to visualize multivariate distances among neighboring neurons and to identify boundaries between clusters within the SOM topology (Fig. 4**)**. This representation provides a complementary view of the SOM structure by highlighting regions of greater dissimilarity in the multidimensional environmental space. Inter-neuron Euclidean distances ranged from 4.48 to 8.52, with a mean of 6.33 (Table 3). The mean silhouette value across samples was 0.261, indicating weak to moderate cluster separation, a value consistent with the presence of a continuous environmental gradient between mangrove regions. The mean Euclidean distance between samples and their respective cluster centers was 3.35 (SD = 1.18), with a maximum of 7.24. Importantly, the minimum inter-cluster distance exceeded the mean sample-to-cluster distance, indicating satisfactory separation among SOM clusters in the multivariate space.

Taken together, these results demonstrate a coherent multivariate differentiation of mangrove environments along the São Paulo coast, with regional patterns emerging from the combined biological, chemical, and sedimentological variables represented in the SOM.

4. Discussion

The main outcome of this study was the identification of a coherent regional gradient of environmental variability across mangrove ecosystems along the southeastern Brazilian coast. This pattern reflects the

Table 2
Descriptive statistics of SOM weights for each input variable after z-score normalization. Mean weight: average value across the six SOM neurons; standard deviation: variability of weights; weight range: difference between maximum and minimum values across neurons. Variable abbreviations follow Table 1.

Variable	Mean Weight	Std Weight	Weight Range
NRRT	−0.0499	0.9343	2.3694
MN	0.0912	0.8677	2.1840
CRAB	0.0466	0.5489	1.6010
Cu.Sed	0.0994	0.9939	2.6977
Pb.Sed	0.0001	1.0559	2.4163
Cd.Sed	0.0012	1.0805	2.2138
Mn.Sed	0.1004	0.9171	2.4882
Cr.Sed	0.0499	0.8670	2.0185
Hg.Sed	0.0163	0.5944	1.6412
CS	−0.0559	0.6332	1.6176
MS	−0.0818	0.7628	2.0753
FS	0.0225	0.9424	2.1799
VFS	0.0215	0.8749	1.9897
SIL	−0.0202	1.0052	2.2521
CLA	−0.0086	0.9058	2.1896
pH	0.0796	0.5890	1.6095
OM	−0.1144	1.0468	2.8116
P	−0.0127	0.8009	1.9540
K	−0.0794	0.7038	1.8215
Ca	−0.0587	0.8785	2.2670
Mg	−0.1272	0.5914	1.5767
Al	−0.1304	0.4167	1.1527
H + Al	−0.1459	0.6329	1.8432
B	−0.1232	0.8455	2.4289
Cu	0.1614	1.1311	2.9232
Fe	−0.0911	0.5828	1.5192
Mn	0.1965	1.1857	3.0908
Zn	0.0457	0.6315	1.7663
S-SO4	−0.1945	0.8427	2.2822

well-established contrast between more-impacted central estuarine systems and relatively well-preserved southern mangroves, while also revealing gradual transitions among adjacent regions.

Recent advances in data-driven and multivariate approaches have expanded the analytical toolkit available for marine and coastal environmental assessment, particularly for interpreting complex ecological datasets (Reichstein et al., 2019; Pourzangbar et al., 2023; Sung et al., 2025; Lai et al., 2026). In mangrove ecosystems, where environmental gradients are often spatially heterogeneous and continuous, such approaches can help identify coherent patterns across biological and geochemical components. In this context, Self-Organizing Maps (SOMs) were applied as an exploratory tool to integrate heterogeneous environmental and biological variables and to identify multivariate patterns that may remain unresolved using conventional linear approaches (Licen et al., 2023; Zhang et al., 2026).

Although cluster separation was moderate (mean silhouette value = 0.261), this pattern is consistent with expectations for natural coastal ecosystems, where environmental gradients tend to be continuous rather than sharply partitioned (Osland et al., 2025). The SOM topology displayed gradual transitions among neighboring neurons rather than abruptly separated clusters, reinforcing the interpretation that mangrove environments along the São Paulo coast are structured by continuous environmental gradients. Notably, the main misclassifications involved Iguape (IGU), Cananéia (CAN), and Juréia (JUR) — geographically adjacent regions along the southern coast — suggesting that the SOM captured a realistic regional environmental gradient rather than producing artificial clusters.

Comparison with Duarte et al. (2016), who applied Principal Component Analysis (PCA) to comparable datasets along the São Paulo coast, reveals strong concordance in identifying regional environmental gradients and conservation status. In that study, biological responses of *Ucides cordatus* closely tracked gradients of sediment quality and metal contamination. Within the multivariate framework applied here, NRRT and MN biomarkers followed the same general contamination gradient but displayed distinct weight distributions across neurons, indicating partially different sensitivities within the multivariate structure. The complete agreement observed for SAV and CUB reinforces SOM's ability to distinguish two regions located within the same estuarine complex. Despite their geographical proximity and hydrological connectivity, these regions are subject to different combinations of environmental pressures. Cubatão is historically influenced by intense industrial activity, whereas São Vicente reflects a mixed scenario involving urban occupation, sewage inputs, and industrial influence. The ability of the SOM to consistently separate these regions suggests that their environmental signatures remain sufficiently distinct to be detected within the multivariate structure of the dataset. Thus, the SOM approach corroborates the main environmental patterns verified by PCA but also improves its interpretative resolution by identifying ecological signatures that are not captured by linear ordinations (Lek et al., 1996; Li et al., 2018; Zhang et al., 2026).

The integrative capacity of the SOM is further illustrated in the spatial differentiation of regions based on sediment-associated metals, where manganese (Mn) and available copper (Cu) showed the greatest variability across the SOM grid. These patterns are consistent with the environmental history and geochemical dynamics of the studied estuarine systems.

Manganese is an essential trace element naturally involved in mangrove biogeochemical cycles and is commonly associated with fine-grained, organic-rich sediments. Its variability may therefore reflect both natural sedimentary processes and anthropogenic inputs. In Iguape, elevated Mn levels are likely associated with the historical legacy of upstream mining activities and the deposition of mining-derived residues, which have been documented in the region for decades (Duarte et al., 2016; CETESB, 2021). Additional contributions may also originate from industrial activities historically established in the central coastal sector, particularly in the Cubatão industrial complex, one of the largest industrial hubs in Latin America.

Copper is likewise an essential trace element, but elevated environmental concentrations are frequently associated with anthropogenic sources, including urban sewage, industrial discharges, port activities, antifouling compounds, and diffuse runoff. In Bertioga, the high variability of Cu may be related to diffuse urban contamination sources, such as untreated sewage and waste disposal, previously reported for the estuary and adjacent channel (Duarte et al., 2016). Similar processes may also contribute to metal enrichment in other sectors of the central coast, including São Vicente, where intense urban occupation and historically limited sewage treatment coverage have been documented.

Together, the combined influence of contaminant sources, sediment deposition processes, estuarine hydrodynamics, and metal retention in fine-grained sediments likely explains why Mn and Cu emerged as major drivers of the environmental gradients identified by the SOM. Conversely, the comparatively narrow weight ranges observed for Al, Fe, and Mg suggest a more homogeneous geochemical background across the studied estuarine systems. Because these elements are commonly associated with the mineral matrix of sediments, their lower contribution to SOM differentiation likely reflects lithogenic control rather than localized anthropogenic inputs.

Biological descriptors also reinforced the integrative capacity of the SOM. The neural grid captured substantial variability in cytotoxic (NRRT) and genotoxic (MN) biomarkers, which displayed relatively high weight amplitudes within the SOM structure. These patterns indicate that physiological stress responses in *U. cordatus* are closely associated with the geochemical gradients identified in the sediment matrix. Importantly, MN and NRRT represent complementary indicators of biological stress: elevated MN frequencies reflect genotoxic impairment associated with contaminant exposure, whereas higher NRRT values indicate greater lysosomal membrane stability and better cellular condition. The reduction in NRRT indicates increased lysosomal membrane permeability, and consequently reduced NRRT values. Furthermore,

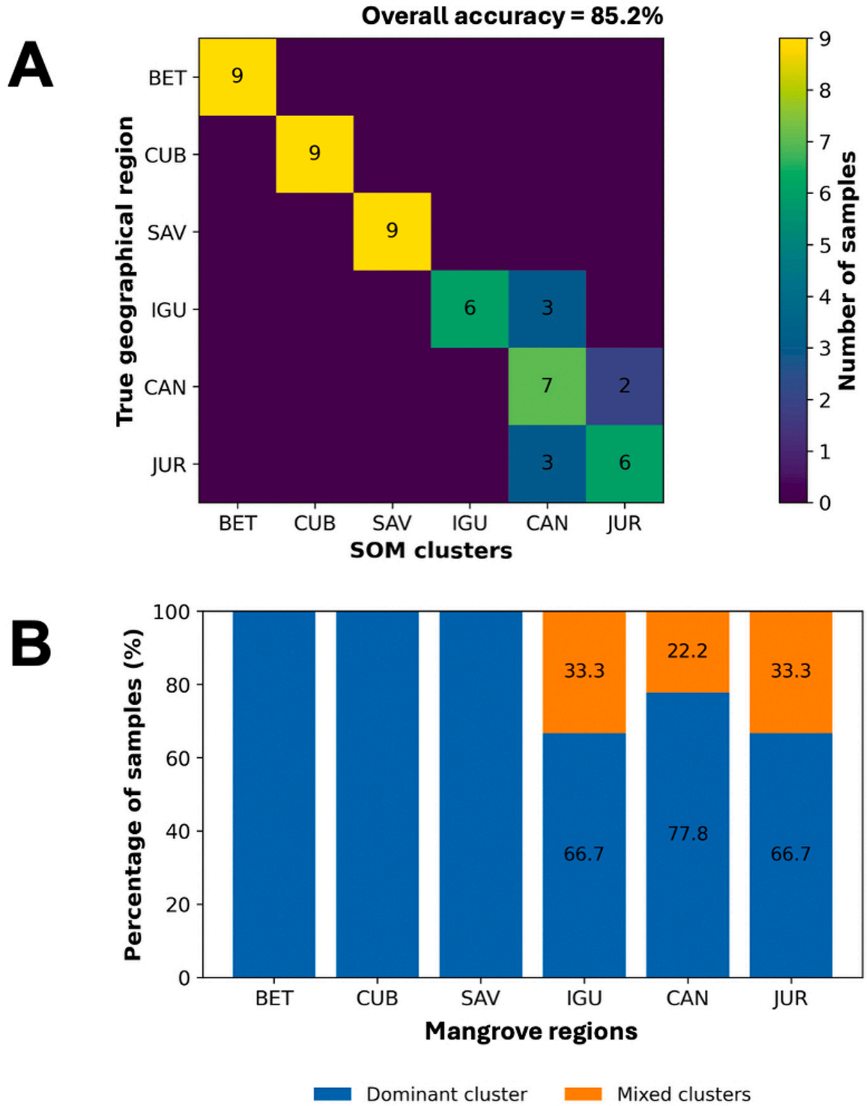

Fig. 3. Classification performance of the Self-Organizing Map (SOM) across the studied mangrove regions. (A) Confusion matrix showing the distribution of samples from each geographical region across SOM clusters. Cell values indicate the number of samples assigned to each cluster. (B) Proportion of samples assigned to dominant (single cluster) and mixed-cluster classifications for each mangrove region.

previous studies have already indicated that contamination by sediment-associated metals, such as Cu and Pb, shows a negative correlation with NRRT variation (Duarte et al., 2017). These metals may induce oxidative stress, leading to lysosomal membrane destabilization, increased membrane permeability, and consequently reduced NRRT values. Different contaminants may preferentially affect distinct physiological pathways. For example, Cu is known to promote the formation of reactive oxygen species, compromising cellular homeostasis and lysosomal integrity, whereas Hg and other genotoxic contaminants may interact more directly with DNA and chromosomal material, increasing the frequency of micronuclei and other nuclear abnormalities. Consequently, NRRT and MN may respond differently to contaminant mixtures, reflecting complementary aspects of biological stress rather than redundant responses. Accordingly, increased MN frequencies may indicate chromosomal damage and interference with cell division, representing a genotoxic pathway distinct from the cytotoxic processes reflected by NRRT, although both may be influenced by metal exposure and other environmental contaminants (Duarte et al., 2017). The partial divergence between these biomarkers within the SOM topology therefore suggests that cytotoxic and genotoxic responses reflect distinct physiological pathways responding to environmental stress, rather than redundant indicators of the same process (van der Oost et al., 2003; Bolognesi and Hayashi, 2011; El-SiKaily and Shabaka, 2024). Unlike cytogenotoxic biomarkers, crab density showed a smaller contribution range, which may be explained by the broader ecological and temporal scales represented by this descriptor. Density is a population-level descriptor shaped by the interaction of several ecological processes (e.g., recruitment, mortality, burrow availability, tidal flooding, and mangrove forest structure; Mota et al., 2023), and therefore tends to respond more slowly to environmental change than cytogenotoxic biomarkers, which provide early-warning signals of physiological stress.

The partial overlap observed among Iguape, Cananéia, and Juréia clusters is consistent with an ecologically meaningful transition rather than a purely methodological limitation (Kohonen, 2001; Legendre and Legendre, 2012; Licen et al., 2023). These regions share similar sedimentary characteristics, geochemical backgrounds, and low levels of anthropogenic influence, resulting in partially overlapping multivariate signatures. Such overlap likely reflects gradual environmental transitions, a pattern frequently reported in SOM-based environmental classifications of heterogeneous coastal systems (Guagliardi et al., 2022).

Distance-based metrics further supported the robustness of the results. The observation that inter-cluster distances exceed the mean

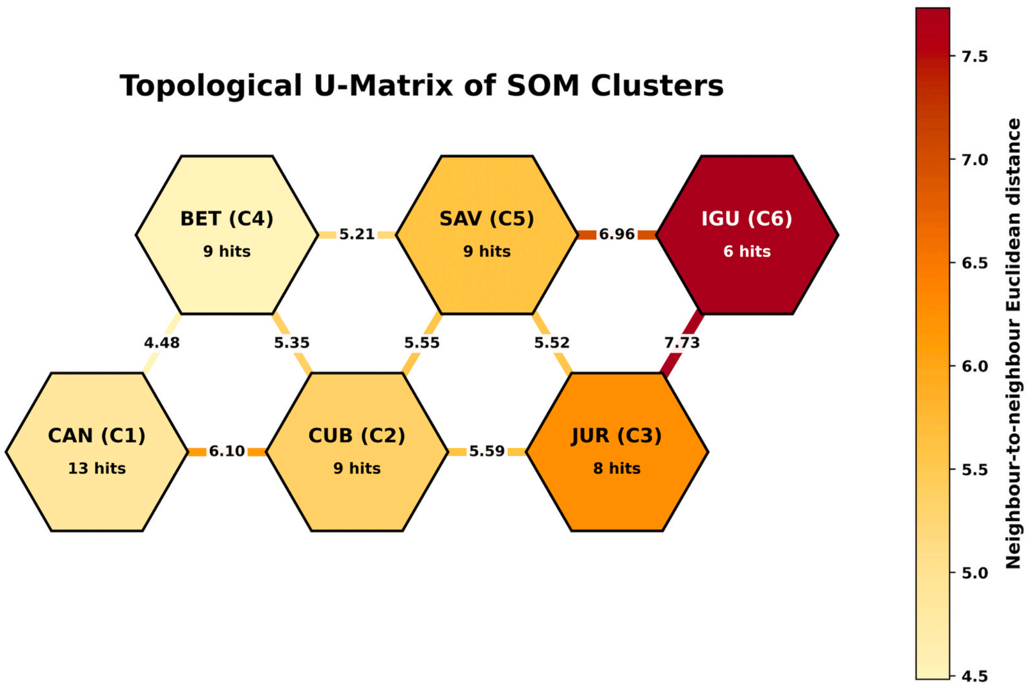

Fig. 4. Topological U-matrix of the six Self-Organizing Map (SOM) clusters derived from 54 samples and 29 biological, chemical, and sedimentological variables. Hexagons represent SOM neurons labelled according to the predominant geographic origin of the samples assigned to each cluster. Numbers inside hexagons indicate the number of hits (samples mapped to each neuron). Colored links between neighboring neurons represent Euclidean distances between the weight vectors of adjacent neurons. Warmer colors indicate greater multivariate dissimilarity and stronger boundaries between clusters, whereas cooler colors indicate higher similarity. Values displayed on each link correspond to the respective inter-neuron Euclidean distance.

Table 3
Inter-neuron Euclidean distances among the six SOM neurons in multidimensional feature space. Higher values indicate greater dissimilarity between neurons.

Neuron	1	2	3	4	5	6
1	0.00	6.10	5.78	4.48	5.15	7.46
2	6.10	0.00	5.59	5.35	5.55	8.18
3	5.78	5.59	0.00	7.30	5.52	7.73
4	4.48	5.35	7.30	0.00	5.21	8.52
5	5.15	5.55	5.52	5.21	0.00	6.96
6	7.46	8.18	7.73	8.52	6.96	0.00

sample-to-cluster distance indicates well-defined environmental groupings while still accounting for local heterogeneity. Samples located farther from cluster centers likely reflect site-specific conditions or transitional environments, which are intrinsic features of mangrove ecosystems. In multivariate environmental analyses, such peripheral samples often indicate localized environmental variability or mixed geochemical signatures within otherwise coherent regional conditions (Hua and Anderson-Frey, 2022; Licen et al., 2023).

From a monitoring perspective, the ability of the SOM to distinguish between stable environmental states and transitional conditions is particularly valuable. Contemporary environmental monitoring increasingly requires analytical tools capable of detecting gradual ecological shifts rather than solely abrupt degradation events (Elliott and Quintino, 2007; Borja et al., 2016; Licen et al., 2023). SOM-based approaches have demonstrated strong potential across a wide range of environmental applications, including soil pollution, aquatic contamination, and sediment quality assessment, by integrating biological and abiotic indicators within a unified analytical framework (Li et al., 2021; Guagliardi et al., 2022; Licen et al., 2023; Li et al., 2025; Zhang et al., 2026).

In addition to its analytical performance, the SOM framework applied here provides practical implications for environmental monitoring in mangrove ecosystems. By integrating sediment geochemistry with physiological biomarkers of *Ucides cordatus*, the neural model allows the identification of multivariate environmental signatures associated with both chronic contamination and relatively preserved conditions. Such integrative approaches are particularly valuable in coastal systems where environmental degradation often occurs gradually and is driven by multiple interacting stressors. In this context, topology-preserving models such as SOMs may help identify early shifts in ecosystem condition before clear ecological thresholds are reached (Scheffer et al., 2015; Borja et al., 2016).

Taken together, these results demonstrate that integrating sediment geochemistry and biological responses provides a robust basis for characterizing environmental variability in mangrove ecosystems. While SOM served as a multivariate analytical tool, the primary drivers of environmental differentiation are linked to sediment contamination processes and their biological consequences.

5. Conclusion

This study demonstrated a coherent regional gradient in environmental variability across mangrove ecosystems along the southeastern Brazilian coast. The observed spatial patterns reflect the contrast between more-impacted central estuarine systems and relatively well-preserved southern mangroves, while also highlighting transitional ecological conditions across adjacent regions.

Sediment geochemistry, particularly trace metal concentrations and associated sediment properties, played a central role in structuring these regional differences. Biological responses in *Ucides cordatus*, as indicated by cytotoxic and genotoxic biomarkers, were closely aligned with these environmental gradients, reinforcing the ecological relevance of this species as a sentinel organism in mangrove ecosystems.

The identification of partial overlap among southern regions indicates that environmental variability in coastal systems is often continuous rather than discrete, underscoring the importance of approaches that can capture transitional conditions.

Although Self-Organizing Maps were used as an exploratory multivariate tool, the primary contribution of this study lies in integrating sediment and biological indicators to describe environmental variability along a regional coastal gradient. Such integrative approaches provide a valuable framework for environmental monitoring, particularly in systems where ecological change occurs gradually and is driven by multiple interacting stressors.

Funding

The authors would like to thank the São Paulo State Research Foundation (FAPESP) for the financial support awarded to MAAP through the "Uçá" III Project (grant # 2009/14725–1), as well as for the Ph.D. scholarship granted to LFAD (grant # 2010/01552–9). The authors are also grateful to the Brazilian National Council for Scientific and Technological Development (CNPq) for the Research Productivity Fellowship awarded to MAAP (grant # 302813/2010–1; triennium 2010–2012). The Article Processing Charge (APC) for publication of this research was funded by the Coordination for the Improvement of Higher Education Personnel (CAPES; ROR identifier: 00x0ma614). For the purpose of Open Access, the authors have applied a Creative Commons Attribution (CC BY) licence to any Author Accepted Manuscript version arising from this submission.

CRediT authorship contribution statement

Marcelo Antonio Amaro Pinheiro: Writing – review & editing, Validation, Supervision, Resources, Project administration, Investigation, Funding acquisition, Data curation, Conceptualization. **Luis Felipe de Almeida Duarte:** Writing – review & editing, Investigation, Data curation. **Caio Rodrigues Nobre:** Writing – review & editing, Investigation. **Esli Emanoel Domingues Mosna:** Writing – review & editing, Investigation. **Rodrigo dos Santos Rodriguez-Lopes:** Writing – review & editing, Investigation. **Todor Petkov:** Writing – review & editing, Visualization, Software, Methodology, Formal analysis. **Aleksandar Dimitrov:** Writing – review & editing, Software, Methodology, Data curation. **Dimitrinka Ivanova:** Writing – review & editing, Writing – original draft, Methodology, Formal analysis, Conceptualization.

Declaration of Competing Interest

The authors declare that they have no known competing financial interests or personal relationships that could have appeared to influence the work reported in this paper.

Acknowledgments

The authors thank the members of the Crustacean Biology Research Group (CRUSTA) for their valuable support during field expeditions and laboratory activities. In addition, the authors are grateful to Gustavo H. S. Pinheiro and EEDM for preparing the map and icons, and for providing photos depicting the mangrove areas investigated in this study. All data were obtained under permanent authorization to collect zoological material granted by the Chico Mendes Institute for Biodiversity Conservation (ICMBio) through SISBIO (permit # 13581–1) to MAAP, as well as authorization from the Scientific-Technical Commission of the São Paulo State Forest Institute (COTEC/FF; SMA process # 260108–009.809/2010) to conduct sample collections in the Juréia-Itatins Ecological Station (JIES).

Appendix A. Supporting information

Supplementary data associated with this article can be found in the online version at doi:10.1016/j.rsma.2026.105255.

Data availability

Data will be made available on request.

References

Adam, M.L., Torres, R.A., Boos, H., Pinheiro, M.A.A., 2023. Espécies sentinelas: monitoramento ambiental com base em biomarcadores de efeito cito- e genotóxico. Rev. CEPSUL - Biodiversidade e Conservação Marinha 12, e20230002. https://doi.org/10.37002/revistacepsul.vol12.2333e20230002.

Albertin-Santos, C.J., Ferreira, G.V.B., Justino, A.K.S., Lucena-Frédou, F., Houllou, L.M., 2025. Does the trophic guild influence microplastic ingestion in nursery areas? Mar. Pollut. Bull. 221, 118559. https://doi.org/10.1016/j.marpolbul.2025.118559.

Alongi, D.M., 2014. Carbon cycling and storage in mangrove forests. Annu. Rev. Mar. Sci. 6, 195–219. https://doi.org/10.1146/annurev-marine-010213-135020.

Atanassov, K., Sotirov, S., 2006. Optimization of a self-organizing map neural network. Adv. Stud. Contemp. Math. 13, 213–220.

Bolognesi, C., Hayashi, M., 2011. Micronucleus assay in aquatic animals. Mutagenesis 26, 205–213. https://doi.org/10.1093/mutage/geq073.

Borja, A., Elliott, M., Andersen, J.H., Berg, T., Carstensen, J., Halpern, B.S., et al., 2016. Integrative assessment of marine systems. Front. Mar. Sci. 3, 20. https://doi.org/10.3389/fmars.2016.00020.

CETESB, 2021. Qualidade das águas costeiras do Estado de São Paulo – 2020. CETESB São Paulo.

Du, X., Niu, D., Chen, Y., Wang, X., Bi, Z., 2022. City classification for municipal solid waste prediction. Waste Manag. 144, 445–453. https://doi.org/10.1016/j.wasman.2022.04.024.

Duarte, L.F.A., Souza, C.A., Nobre, C.R., Pereira, C.D.S., Pinheiro, M.A.A., 2016. Multi-level biological responses in *Ucides cordatus* as indicators of conservation status in mangrove areas. Ecotoxicol. Environ. Saf. 133, 176–187. https://doi.org/10.1016/j.ecoenv.2016.07.018.

Duarte, L.F.A., Souza, C.A., Pereira, C.D.S., Pinheiro, M.A.A., 2017. Metal toxicity assessment by sentinel species of mangroves. Ecotoxicol. Environ. Saf. 145, 367–376. https://doi.org/10.1016/j.ecoenv.2017.07.051.

Duarte, L.F.A., Moreno, J.B., Catharino, M.G.M., Moreira, E.G., Trombini, C., Pereira, C.D.S., 2019. Mangrove metal pollution induces biological tolerance to Cd in a crab sentinel species subpopulation. Sci. Total. Environ. 687, 768–779. https://doi.org/10.1016/j.scitotenv.2019.06.039.

Duarte, L.F.A., Ortega, A.S.B., Paço, M.S., Nobre, C.R., Sadauskas-Henrique, H., Gusso-Choueri, P.K., et al., 2025. Coastal fallout of settleable particulate matter: metal bioaccumulation and sublethal toxicity in estuarine bivalves. Mar. Pollut. Bull. 220, 118441. https://doi.org/10.1016/j.marpolbul.2025.118441.

Duke, N.C., Meynecke, J.O., Dittmann, S., Ellison, A.M., Anger, K., Berger, U., et al., 2007. A world without mangroves? Science 317, 41–42. https://doi.org/10.1126/science.317.5834.41b.

Elliott, M., Quintino, V., 2007. The estuarine quality paradox. Mar. Pollut. Bull. 54, 640–645. https://doi.org/10.1016/j.marpolbul.2007.02.003.

El-SiKaily, A., Shabaka, S., 2024. Biomarkers in aquatic systems: advancements and applications. Egypt. J. Aquat. Res. 50, 169–182. https://doi.org/10.1016/j.ejar.2024.05.002.

Friess, D.A., Rogers, K., Lovelock, C.E., Krauss, K.W., Hamilton, S.E., Lee, S.Y., et al., 2019. The state of the world's mangrove forests: past, present, and future. Annu. Rev. Environ. Resour. 44, 89–115. https://doi.org/10.1146/annurev-environ-101718-033302.

Fusco, G., Perez, J., 2019. Bayesian network clustering and self-organizing maps: a comparison. Cybergeo 887. https://doi.org/10.4000/cybergeo.31909.

Gonçalves, W.F.O., Luiz-Silva, W., Machado, W., Nizoli, E.C., Santelli, R.E., 2012. Geochemistry of intertidal sediment pore waters in an industrialized estuary. An. Acad. Bras. Ciênc. 84, 427–442. https://doi.org/10.1590/S0001-37652012005000021.

Guagliardi, I., Astel, A.M., Cicchella, D., 2022. Exploring soil pollution patterns using self-organizing maps. Toxics 10, 416. https://doi.org/10.3390/toxics10080416.

Hagan, M.T., Demuth, H.B., Beale, M.H., de Jesús, O., 2014. Neural network design. Oklahoma State University, Stillwater.

Heck, N., Goldberg, L., Andradi-Brown, D.A., Campbell, A., Narayan, S., Ahmadia, G.N., et al., 2024. Global drivers of mangrove loss in protected areas. Conserv. Biol. 38, e14293. https://doi.org/10.1111/cobi.14293.

Hua, Z., Anderson-Frey, A.K., 2022. Self-organizing maps for classification of tornado-favorable conditions. Mon. Weather. Rev. 150, 393–407. https://doi.org/10.1175/MWR-D-21-0168.1.

Hussain, M., Liu, S., Hussain, W., Liu, Q., Hussain, H., Ashraf, U., 2024. Deep learning for reservoir porosity prediction and SOM for lithofacies. J. Appl. Geophys. 230, 105502. https://doi.org/10.1016/j.jappgeo.2024.105502.

IUCN, 2024. More than half of all mangrove ecosystems at risk of collapse by 2050. https://iucn.org/press-release/202405/more-half-all-mangrove-ecosystems-risk-collapse-2050-first-global-assessment (accessed 28 January 2025).

Khan, W.R., Mohamad, A.L., Ibrahim, F.H., 2025. Biodiversity, health, and ecosystem services of mangroves. Forests 16, 1278. https://doi.org/10.3390/f16081278.

Kim, B.S.M., Trevizani, T.H., Benedetti, B., Angeli, J.L.F., Siegle, E., Mahiques, M.M., et al., 2022. Mercury distribution in sediments from the Santos–São Vicente estuarine system. J. Trace Elem. Miner. 2, 100008. https://doi.org/10.1016/j.jtemin.2022.100008.

Kohonen, T., 2001. Self-organizing maps. Springer, Berlin, Heidelberg. https://doi.org/10.1007/978-3-642-56927-2.

Kristensen, E., 2008. Mangrove crabs as ecosystem engineers, with emphasis on sediment processes. J. Sea Res. 59, 30–43. https://doi.org/10.1016/j.seares.2007.05.004.
Lai, X., Xu, N., Jiang, J., Jia, J., Liu, Y., Su, Y., et al., 2026. Machine learning-informed vulnerability assessment of coastal erosion. J. Hydrol. Reg. Stud. 64, 103132. https://doi.org/10.1016/j.ejrh.2026.103132.
Legendre, P., Legendre, L., 2012. Numerical ecology, third ed. Elsevier, Amsterdam.
Lek, S., Delacoste, M., Baran, P., Dimopoulos, I., Lauga, J., Aulagnier, S., 1996. Neural networks in ecology. Ecol. Model. 90, 39–52. https://doi.org/10.1016/0304-3800(95)00142-5.
Li, J., Li, X., Tai, X.S., Tuo, X.Y., Zhou, F.Y., Rong, Y.J., et al., 2025. Machine learning-assisted source identification of heavy metals. Sci. Rep. 15, 17451. https://doi.org/10.1038/s41598-025-02307-1.
Li, K., Sward, K., Deng, H., Morrison, J., Habre, R., Franklin, M., et al., 2021. Diurnal environmental exposure patterns using SOM. Sci. Rep. 11, 24052. https://doi.org/10.1038/s41598-021-03515-1.
Li, T., Sun, G., Yang, C., Liang, K., Ma, S., Huang, L., 2018. Using self-organizing maps for coastal water quality classification. Sci. Total. Environ. 628–629, 1446–1459. https://doi.org/10.1016/j.scitotenv.2018.02.163.
Licen, S., Astel, A., Tsakovski, S., 2023. Self-organizing map algorithm for pollutant patterns: a review. Sci. Total. Environ. 878, 163084. https://doi.org/10.1016/j.scitotenv.2023.163084.
Mahiques, M.M., Burone, L., Figueira, R.C.L., Lavenére-Wanderley, A.A.O., Capellari, B., Rogacheski, C.E., et al., 2009. Anthropogenic influences in a lagoonal environment: a multiproxy approach. Braz. J. Oceanogr. 57, 325–337. https://doi.org/10.1590/S1679-87592009000400007.
Marchand, C., Lallier-Vergès, E., Baltzer, F., Albéric, P., Cossa, D., Baillif, P., 2006. Heavy metals distribution in mangrove sediments. Mar. Chem. 98, 1–17. https://doi.org/10.1016/j.marchem.2005.06.001.
Millo, C., Bravo, C., Covelli, S., Pavoni, E., Petranich, E., Contin, M., et al., 2021. Metal binding and sources of humic substances in estuarine sediments. Appl. Sci. 11, 8466. https://doi.org/10.3390/app11188466.
Mota, T.A, Pinheiro, M.A.A., Evangelista-Barreto, N.S., Rocha, S.S., 2023. Density and extractive potential of "uçá"-crab, *Ucides cordatus* (Linnaeus, 1763), in mangroves of the "Todos os Santos" Bay, Bahia, Brazil. Fish. Res. 265, 106733.
N'goran, P.D.A., Diabate, D., Kouassi, N.L.B., Yao, K.M., Kinimo, K.C., Ouattara, A.A., et al., 2022. Geochemical speciation and distribution of trace metals in sediments around gold mining areas in Côte d'Ivoire. Environ. Earth Sci. 81, 333. https://doi.org/10.1007/s12665-022-10447-0.
Osland, M.J., Bradford, J.B., Toth, L.T., Germino, M.J., Grace, J.B., Drexler, J.Z., et al., 2025. Ecological thresholds and transformations due to climate change. Ecosphere 16, e70229. https://doi.org/10.1002/ecs2.70229.
Perina, F.C., Abessa, D.M.S., 2020. Contamination and toxicity in a subtropical estuarine protected area. Ocean. Coast. Res. 68, e20313. https://doi.org/10.1590/s2675-28242020068313.
Pinheiro, M.A.A., 2026. Biologia e ecologia do caranguejo-uçá. In: Masuda, L.S.M., Andrade, D.F.C., Chaves, F.O., Mendes, K.R., Reis, L.M.A., Pinheiro, M.A.A., et al. (Eds.), Programa Nacional de Monitoramento da Biodiversidade, 3. ICMBio, Brasília, pp. 36–90.
Pinheiro, M.A.A., Fiscarelli, A., Hattori, G.Y., 2005. Growth of the mangrove crab *Ucides cordatus*. J. Crustac. Biol. 25, 293–301. https://doi.org/10.1651/C-2438.
Pinheiro, M.A.A., Duarte, L.F.A., Toledo, T.R., Adam, M.L., Torres, R.A., 2013. Habitat monitoring and genotoxicity in *Ucides cordatus*. Environ. Monit. Assess. 185, 8273–8285. https://doi.org/10.1007/s10661-013-3172-9.
Pinheiro, M.A.A., Souza, C.A., Zanotto, F.P., Torres, R.A., Pereira, C.D.S., 2017. The crab *Ucides cordatus* and related taxa as environmental sentinels. In: Larramendy, M.L. (Ed.), Ecotoxicology and genotoxicology: non-traditional aquatic models. Royal Society of Chemistry, London, pp. 212–242. https://doi.org/10.1039/9781782629887-00212.
Pinheiro, M.A.A., Kriegler, N., Souza, C.A., Duarte, L.F.A., 2021. Feeding habits influence baseline micronuclei frequency in crabs. Wetlands 41, 30. https://doi.org/10.1007/s13157-021-01427-4.
Pinheiro, M.A.A., Souza, F.V.B., Boos, H., Duarte, L.F.A., 2022. Cytotoxicity, genotoxicity, and population impacts in *Ucides cordatus* after an environmental disaster. Nauplius 30, e2022025. https://doi.org/10.1590/2358-2936e2022025.
Pourzangbar, A., Jalali, M., Brocchini, M., 2023. Machine learning in marine and coastal modelling: a review. Front. Environ. Eng. 2, 1235557. https://doi.org/10.3389/fenve.2023.1235557.
R Core Team, 2024. R: a language and environment for statistical computing. R Foundation, Vienna. https://www.r-project.org/.
Ramos, M.A.V., Rocha, S.S., Winkaler, E.U., Nobrega, G.N., Carvalho, J.C., Souza Santos, A.Z., et al., 2024. Soil contamination and biomarkers in *Ucides cordatus* in mangroves from Baía de Todos os Santos, Brazil. Water Air Soil. Pollut. 235, 218. https://doi.org/10.1007/s11270-024-07037-0.
Reichstein, M., Camps-Valls, G., Stevens, B., Jung, M., Denzler, J., Carvalhais, N., et al., 2019. Deep learning for Earth system science. Nature 566, 195–204. https://doi.org/10.1038/s41586-019-0912-1.
Rinehart, S.A., Dybiec, J.M., Walker, J.B., Simpson, L., Cherry, J.A., 2024. Effects of burrowing crabs on coastal sediments and their functions: a systematic meta-analysis. Ecosphere 15, e4927. https://doi.org/10.1002/ecs2.4927.
Schaeffer-Novelli, Y., Abuchahla, G.M.D.O., Cintrón-Molero, G., 2023. Brazilian mangroves and salt marshes. Springer International Publishing, Cham. https://doi.org/10.1007/978-3-031-13486-9.
Scheffer, M., Carpenter, S.R., Dakos, V., van Nes, E.H., 2015. Indicators of ecological resilience and critical transitions. Annu. Rev. Ecol. Evol. Syst. 46, 145–167. https://doi.org/10.1146/annurev-ecolsys-112414-054242.
Sotirov, S., Krawczak, M., Petkova, D., Atanassov, K., 2023. Intuitionistic fuzzy neural network with filtering functions. Notes Intuit. Fuzzy Sets 29, 231–238. https://doi.org/10.7546/nifs.2023.29.2.231-238.
Souza, C.A., Duarte, L.F.A., João, M.C.A., Pinheiro, M.A.A., 2018. Biodiversidade e conservação dos manguezais: importância bioecológica e econômica. In: Pinheiro, M.A.A., Talamoni, A.C.B. (Eds.), Educação ambiental sobre manguezais. UNESP, São Vicente, pp. 16–56.
Souza, F.V.B., Pinheiro, M.A.A., 2022. Biology, trophic chain, and ethnobiological calendar of the mangrove crab *Ucides cordatus* (Linnaeus, 1763). Nauplius 30, e2022017. https://doi.org/10.1590/2358-2936e2022017.
Sung, T., Kim, S.-H., Sim, S., Han, D., Jang, E., Im, J., 2025. High-resolution sea surface salinity estimation using machine learning. Int. J. Appl. Earth Obs. Geoinf. 137, 104427. https://doi.org/10.1016/j.jag.2025.104427.
Swetha, S., Veerasingam, S., Rajendran, S., Hassan, H., Hashmi, M.Z.U.R.R., Alsaadi, H., et al., 2025. Long-term trends in heavy metal contamination of marine sediments in the Arabian Gulf: a meta-analysis. Environ. Monit. Assess. 197, 873. https://doi.org/10.1007/s10661-025-14348-0.
Timoszczuk, C.T., Taniguchi, S., Kim, B.S.M., Martins, C.C., Lourenço, R.A., Figueira, R.C.L., et al., 2026. Organic biomarkers as indicators of contamination in a subtropical estuary. Reg. Stud. Mar. Sci. 93, 104698. https://doi.org/10.1016/j.rsma.2025.104698.
Tognella, M.M.P., Falqueto, A.R., Espinoza, H.D.C.F., Gontijo, I., Gontijo, A.B.P.L., Fernandes, A.A., et al., 2022. Mangroves as traps for environmental damage to metals: the case study of the Fundão Dam. Sci. Total. Environ. 806, 150452. https://doi.org/10.1016/j.scitotenv.2021.150452.
van der Oost, R., Beyer, J., Vermeulen, N.P., 2003. Fish bioaccumulation and biomarkers in environmental risk assessment. Environ. Toxicol. Pharmacol. 13, 57–149. https://doi.org/10.1016/S1382-6689(02)00126-6.
Wehrens, R., Buydens, L.M.C., 2007. Self- and super-organizing maps in R. J. Stat. Softw. 21, 1–19. https://doi.org/10.18637/jss.v021.i05.
Wehrens, R., Kruisselbrink, J., 2023. kohonen: self-organizing maps. R package version 3.0.12. https://cran.r-project.org/package=kohonen.
Zhang, J., Qian, H., Gao, Y., Xu, X., Shi, Z., Cao, Z., et al., 2026. Identification of heavy metal sources using SOM and statistical methods. J. Environ. Chem. Eng. 14, 121889. https://doi.org/10.1016/j.jece.2026.121889.
Zhang, Z.-X., Sachs, J.P., Wang, Y.-P., Chen, Z.L., Huguet, A., He, D., 2025. Molecular and trace metal signatures of pristine and anthropogenically altered mangrove sediments. Mar. Pollut. Bull. 219, 118309. https://doi.org/10.1016/j.marpolbul.2025.118309.